Supporting Information

Tuning Interfacial Electrical Field of Bipolar Membranes with Temperature and Electrolyte Concentration for Enhanced Water Dissociation

Huanlei Zhang[1,2,†], *Dongbo Cheng*[1,2,†], *Chengxiang Xiang*[3], *Meng Lin*[1,2,*]

[1] Department of Mechanical and Energy Engineering, Southern University of Science and Technology, Shenzhen 518055, China

[2] SUSTech Energy Institute for Carbon Neutrality, Southern University of Science and Technology, Shenzhen 518055, China

[3] Liquid Sunlight Alliance, Department of Applied Physics and Material Science, California Institute of Technology, Pasadena, California 91125, United States

† contributed equally to this work

Corresponding Author: linm@sustech.edu.cn

This file includes:

Total – 17 pages, 13 figures, and 1 table

Figure S1-S13, Table S1

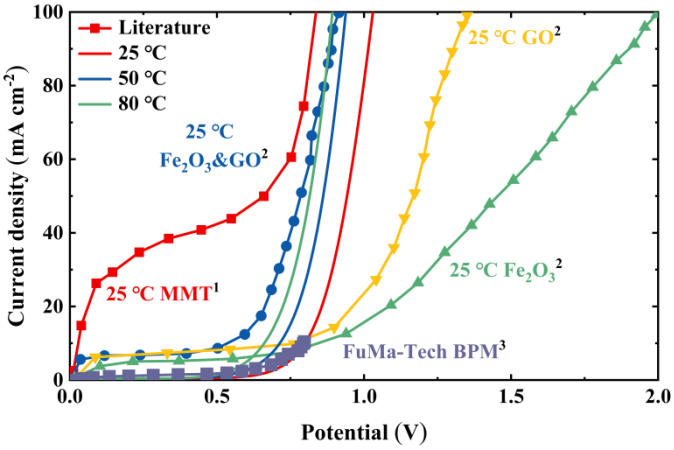

Figure S1. IV curves comparison with various literature data.

The dielectric constant was estimated using $\varepsilon_{sol} = \varepsilon_W - \beta_c c_{sol} \varepsilon_0$ (eq. 21), in which β_c is solution dependent.[4] In the reference[5], β_c is 12.5% lower for K^+ compared to Na^+ based electrolyte. Note that the electrolyte discussed in reference[4] was KCl and NaCl and we assumed the dielectric constant difference was induced by the cations. We performed additional calculations with different diffusion coefficients and dielectric constants (see Figure S2). We observe no difference when using two different electrolytes.

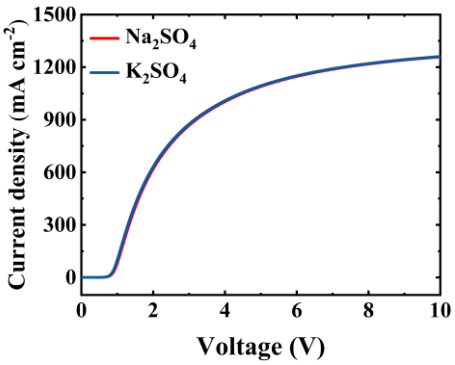

Figure S2. Comparison between Na_2SO_4 and K_2SO_4 with different diffusion coefficients and dielectric constants.

Experimental Methods for 4-Probe Measurement

BPM voltage measurements were performed in a H type cell. The Keithley 2601B (V/I range 100 fA - 10A, 100 nV - 40 V, accuracy 0.015%) was used as the power supply. The BPM (Fumatech) voltage drop was determined by measuring the voltage difference between two Ag/AgCl reference electrodes (4 M KCl). The temperature of electrolyte was measured through two K-type thermocouples (range 0 ~ 1000 ºC, ±2 K). The Keithley DAQ6510 (V/I range 100 pA - 3A, 100 nV - 1000 V, accuracy < 0.015%) was used for the data acquisition of voltage and temperatures. Na_2SO_4 (Aladdin, AR, 99%) used as the catholyte and the anolyte was flowed to the H type cell at a flow rate of 25.5 mL min^{-1} with the control of peristaltic pump (Longer Pump, BT100-2J, 0.1rpm – 100rpm, accuracy = 0.1rpm), and the temperature of the electrolyte with the control of the right water bath. The BPM voltages were measured in the multistep chronopotentiometry mode and the applied current density was swept from low current density to high current density. The voltage at each applied current density was recorded once the voltage stabilized (typical after 5 mins). The hot water with the control of left water bath was flowed to the insulation layer of H type cell at a rate of 1090 mL min^{-1} using peristaltic pump (Kamoer, KKDD-24B17 A, flow rate >840 ml/min). The temperature of electrolyte was heated by hot water and stabilized at 25 ºC, 50 ºC, and 80 ºC (see Figure S3).

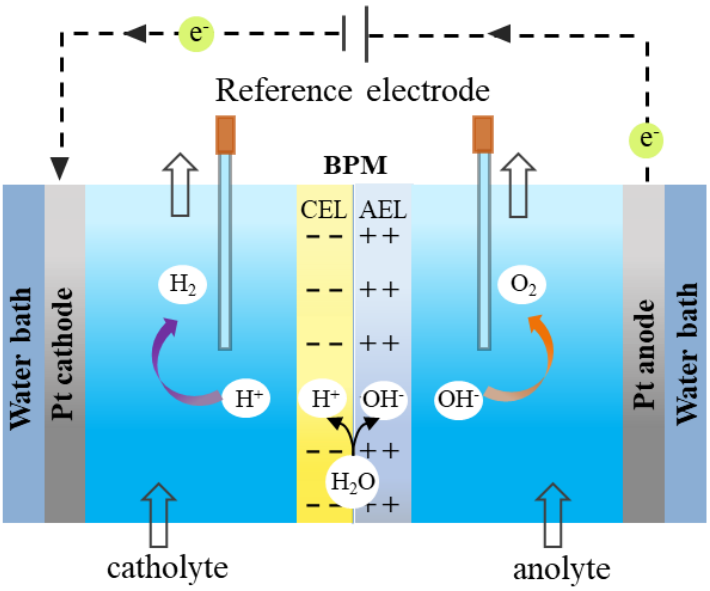

Figure S3. Schematic illustration of the Experimental setup consisting of water bath, Platinum (Pt) electrodes, catholyte compartment, BPM, and anolyte compartment. The anolyte and catholyte were 1 M Na_2SO_4 and BPM with an active area of 1.0 cm^2.

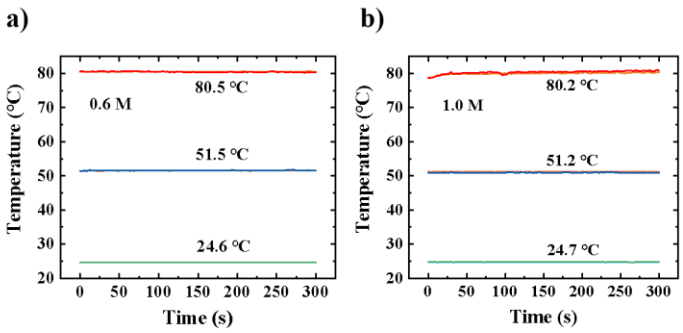

Figure S4. The temperature of electrolyte with concentration of (a) 0.6 M and (b) 1.0 M stabilized at 25 ºC, 50 ºC, and 80 ºC.

Higher IEC value leads to better performing BPM due to enhanced junction electrical field. However, the IEC value do not change the trend of the BPM performance and hence not changing the conclusions of this study. The detailed effect of IEC can be found in our previous work.[6]

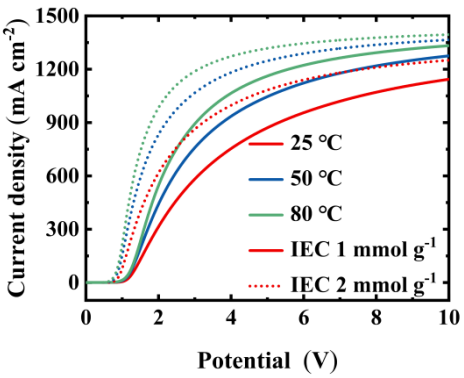

Figure S5. IV curves for different temperature with IEC is 1 mmol g^{-1} (solid lines) and 2 mmol g^{-1} (dash lines).

Table S1. Water Transport Parameters in BPM

Property	Value	Unit
D_W	$0 < \lambda < 4$: $7.32\times10^{-8}\exp(0.12\lambda)+5.41\times10^{-10}\exp(1.44\lambda)\exp\left(-\frac{2436[\mathrm{K}]}{T}\right)+2\times10^{-23}\left(\frac{T}{1[\mathrm{K}]}\right)^{5.2796}$ $4 \le \lambda \le 22$: $1.58\times10^{-8}\exp(-4.66\lambda)+1.45\times10^{-7}\exp(10.04\lambda)\exp(-)\frac{2436[\mathrm{K}]}{T}+2\times10^{-23}\left(\frac{T}{1[\mathrm{K}]}\right)^{5.2796}$	$m^2\ s^{-1}$
ξ_W	25 °C - 1.4 50 °C - 2.4 80 °C - 4.1	1

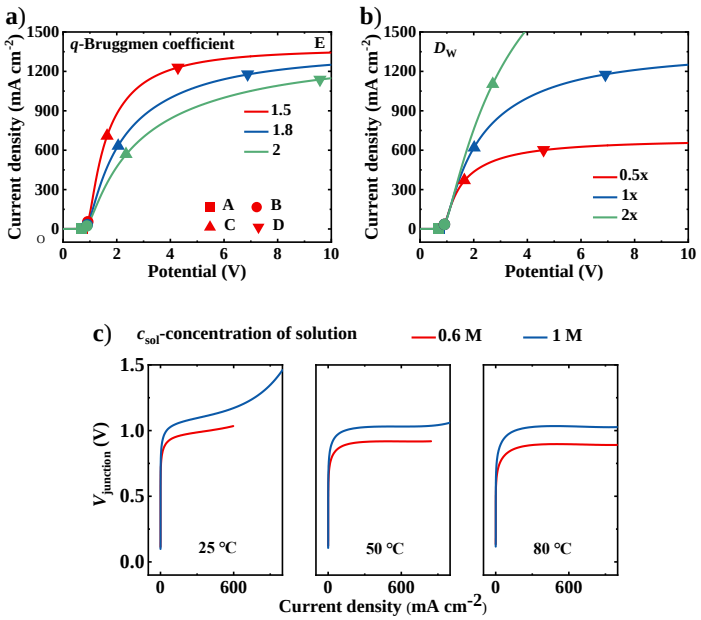

Figure S6. (a) *IV* curves for different Bruggman coefficients. (b) *IV* curves for different diffusion coefficients of water. (c) Potential drop of junction (V_{junction}) as a function of current density at different temperatures and different c_{sol}.

The effective diffusion coefficient of each ion species (D_i^{eff}) depends on the phase. In the aqueous electrolyte phase, these diffusion coefficients are equal to their values in pure water. The Bruggman relation was used within the bipolar membrane ($D_i^{\text{eff}} = D_i f_{\text{mem}}{}^q$). Here f_{mem} is the porosity of the membrane (0.15), q is Bruggman coefficient in the model. Regarding the effect of electrolyte concentration on the q

during BPM operation, the current research data is lacking, and the internal mechanism is not clear. This study did not explore this in depth. q is corrected by passing through our experimental data. In this study, it is set to 1.8 when the electrolyte concentration is 1 M, and it is set to 1.6 when the electrolyte concentration is 0.6 M.

Figure S6a shows the *IV* curves for different q. It can be shown that the change of q affects the slope of the B-C region (ohmic region). Figure 2b shows the B-C region (ohmic region) of the *IV* curve of simulation and experiment, which can be completely corresponded. At the same time, the change of q will also affect the D-E region (Water-limiting region). Compared with q, the change of D_W does not affect the *IV* curve of B-C region (ohmic region). But it will affect D-E region (Water-limiting region).

In order to fit the experimental data, the q was adjusted from 1.8 to 1.6 when the electrolyte concentration changed. Figure 5a shows that the experimental data of c_{sol}=0.6 M and c_{sol}=1 M at different temperatures are basically consistent with the simulated data, which proves that the model developed in this study has universal applicability of temperature and concentration. In addition, the decrease of the solution concentration has an effect on the ohmic limit stage, which is the decrease of the $V_{junction}$ voltage (see Figure S6c).

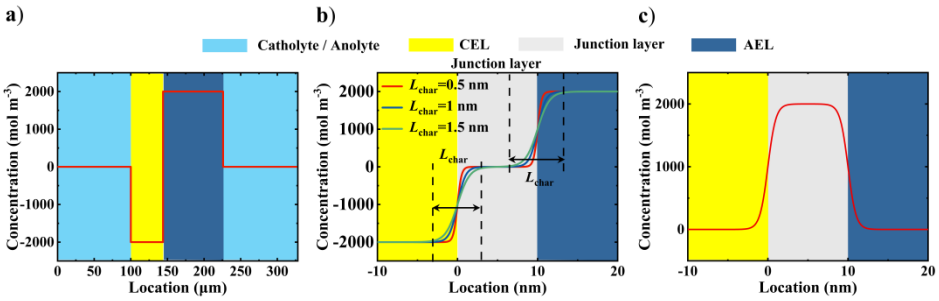

Figure S7. (a) Fixed charge concentration as a function of location over the entire calculation domain. (b) Zoom in fixed charge concentration profiles and catalyst concentration profiles (c) for the junction layer with its adjacent AEL and CEL regions (10 nm for each) at different L_{char}.

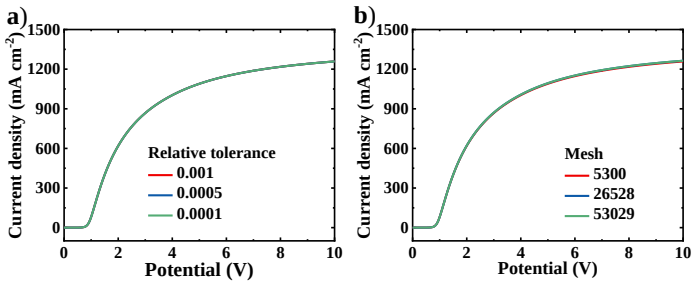

Figure S8. (a) *IV* curves for different relative tolerance of solver. (b) *IV* curves for different mesh elements.

The IV curves are almost the same for different relative tolerances and different mesh elements. Decreasing the relative tolerance or increasing the elements of meshes has little effect on the accuracy of the results, justifying our choice of relative tolerance and number of meshes.

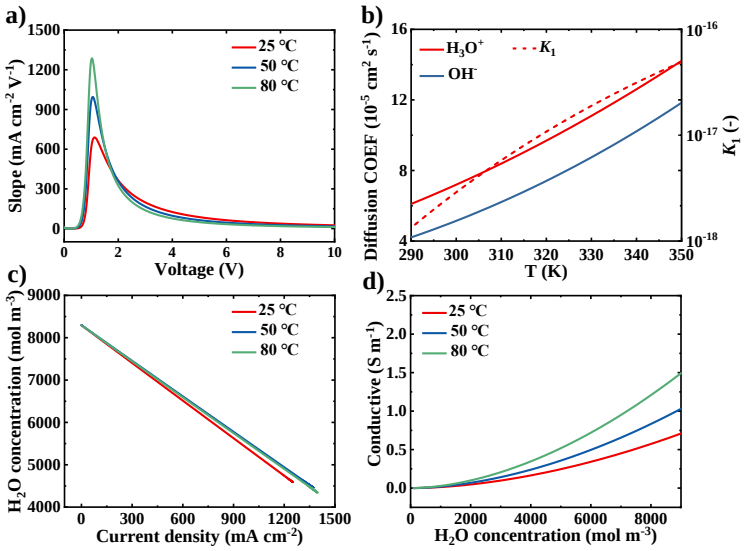

Figure S9. (a) The slope of the *IV* curve at different temperatures. (b) Ions diffusion coefficient and WD equilibrium constant as a function of temperature. (c) Average water concentration in the bipolar membrane as a function of current density at different temperatures. (d) Conductivity of a 1 M Na_2SO_4 solution as a function of water concentration.

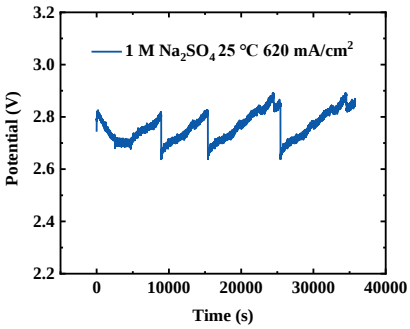

Figure S10. Long time (>10 hours) test of BPM performance at 25 ºC, current density 620 mA cm^{-2}, 1 M Na_2SO_4.

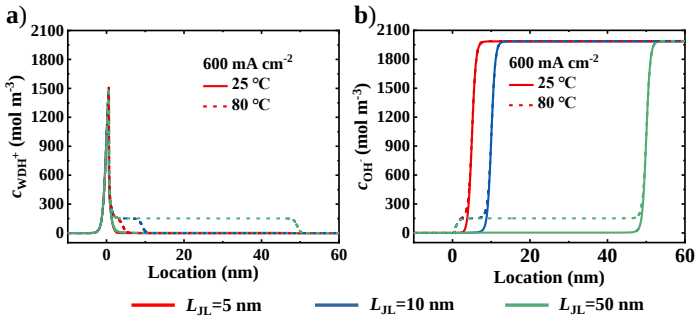

Figure S11. (a) WDH^+ concentration profiles and (b) OH^- concentration profiles at the junction layer for various junction layer thicknesses and temperatures at 600 mA cm^{-2}. Solid lines are for 25 °C and dashed lines for 80 °C.

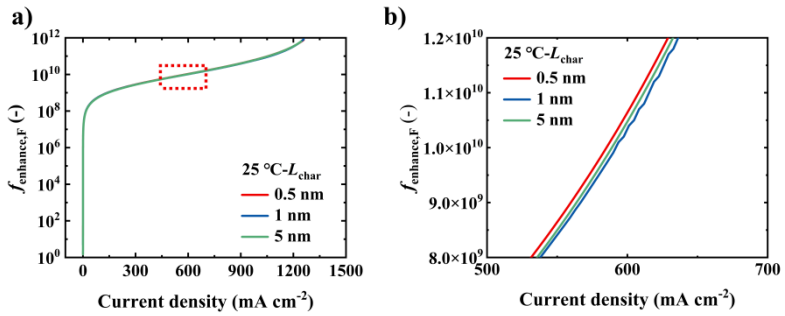

Figure S12. (a) The enhancement factor $f_{electrical,F}$ for reaction 1 due to electric field increase as a function of current density at various L_{char}. (b) Zoom in sub figure for the current density in the range of 500 - 700 mA cm $^{-2}$.

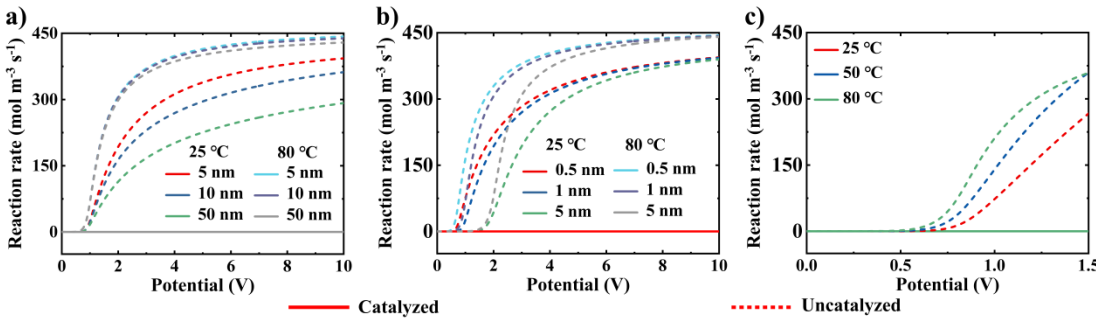

Figure S13. (a) The simulation contribution of catalyzed pathway and uncatalyzed pathway of WD as a function of voltage across the BPM at different junction layer thickness, (b) different abruptness. (c) different solution concentration.

References

(1) Eswaraswamy, B.; Suhag, A.; Goel, P.; Chattopadhyay, S. Potential of montmorillonite nanoclay as water dissociation catalyst at the interface of bipolar membrane. Separation and Purification Technology. 2022, 295, 121257, DOI 10.1016/j.seppur.2022.121257.

(2) Kim, B. S.; Park, S. C.; Kim, D. H.; Moon, G. H.; Oh, J. G.; Jang, J.; Kang, M.; Yoon, K. B.; Kang, Y. S. Bipolar Membranes to Promote Formation of Tight Ice-Like Water for Efficient and Sustainable Water Splitting. Small. 2020, 16, 2002641, DOI 10.1002/smll.202002641.

(3) Vermaas, D. A.; Wiegman, S.; Nagaki, T.; Smith, W. A. Ion transport mechanisms in bipolar membranes for (photo) electrochemical water splitting. Sustainable Energy Fuels. 2018, 2, 2006-2015, DOI 10.1039/C8SE00118A.

(4) Gavish, N.; Promislow, K. Dependence of the dielectric constant of electrolyte solutions on ionic concentration: A microfield approach. Physical review E. 2016, 94, 012611, DOI 10.1103/PhysRevE.94.012611.

(5) Haggis, G. H.; Hasted, J. B.; Buchanan, T. J. The dielectric properties of water in solutions. The Journal of Chemical Physics. 1952, 20, 1452-1465, DOI 10.1063/1.1700780.

(6) Lin, M.; Digdaya, I. A.; Xiang, C. Modeling the electrochemical behavior and interfacial junction profiles of bipolar membranes at solar flux relevant operating current densities. Sustainable Energy Fuels. 2021, 5, 2149-2158, DOI 10.1039/D1SE00201E.